

Effect of Microstructure on Corrosion Resistance of Pipelines Steels Buried in Alkaline Soil

S. BRICK CHAOUCHE

Laboratory Research Methods of Industrial Engineering-Environment

Faculty of Mechanical Engineering –Process Engineering, USTHB BP. 32 - EL ALIA 16110 - BAB EZZOUAR
- ALGER – ALGERIA

Brick_chaouche@hotmail.com

A. LOUNIS

Laboratory Science and Engineering Materials

Faculty of Mechanical Engineering –Process Engineering, USTHB BP. 32 - EL ALIA 16110 - BAB
EZZOUAR - ALGER – ALGERIA

zlounis@yahoo.com

K. TAIBI

Laboratory Science and Engineering Materials

Faculty of Mechanical Engineering –Process Engineering, USTHB BP. 32 - EL ALIA 16110 - BAB
EZZOUAR - ALGER – ALGERIA

kameltaibi@yahoo.fr

G. NEZZAL

Laboratory Research Methods of Industrial Engineering-Environment

Faculty of Mechanical Engineering –Process Engineering, USTHB BP. 32 - EL ALIA 16110 - BAB EZZOUAR
- ALGER – ALGERIA

ghania.nezzal@enp.edu.dz

Abstract

In this work, we tried to examine the effect of microstructure of low carbon pipeline steels on their behavior to corrosion when they are buried in alkaline soil. In this environment, the corrosion rate of these steels depends on a number of different parameters. Perhaps the most significant of these parameters, however, is the formation, evolution and nature of the corrosion products which are deposited on the metal surface. The laboratory experiments realized from electrochemical measurements and characterization of corrosion products have shown that the microstructure influences the properties of the corrosion layers, such as morphology, proportion of the various chemical compounds present, adherence of the film, and the protective properties. The results obtained are striking, not only was there a difference in certain properties of corrosion layers, but their protective power is strongly affected.

Keywords microstructure, low carbon line pipe steel, corrosion products, corrosion rate, alkaline soil

Introduction

Carbon steel used in oil and gas transport, are manufactured according to the American Petroleum Institute (API) specifications 5L, and they don't have a closely specified elemental composition and microstructure. Consequently, they are fabricated for a set of

mechanical requirements such as yield strength, tensile strength and fracture toughness. This can allow for significant variations of the elemental composition and microstructure, which can also influence corrosion performance [1]. Generally, the final microstructure and mechanical properties of carbon steel pipes are determined by its chemical compositions and thermomechanical treatments used during the production processes. Similarly, they can vary significantly between pipes of the same grade from different manufacturers, and these variations can lead to substantial differences in the corrosion resistance. When they are buried in the soil, these pipes are, generally, protected from the external aggressions by a bituminous coating whose action is coupled with a cathodic protection system. Unfortunately, corrosion and cracking problems still can occur in the system under certain conditions. The corrosion rate of these pipes varies according to a host of different parameters. The most Significant of these parameters, however, is the formation, evolution and nature of the corrosion products which are deposited on the metal surface.

The influence of passive layer on the steel corrosion is through a physical blocking effect that inhibits the access of corrosive species; it can completely stop, or accelerated the corrosion process. Therefore, the nature of the layer of deposit is the main factor influencing the protective of steel. It was necessary to know more about the structure and properties of passive film. A considerable number of investigations have been devoted to the study of the electronic properties and chemical compositions of passive films, particularly, on steel [2-10]. Others have studied the effect of various parameters such as pH, oxygen levels, humidity, composition of the electrolyte on the mechanism formation and transformation of the oxides and hydroxides, particularly in soil [11-13]. But little works has addressed the influence of microstructure, on the formation of iron oxides, and on their inhibitory properties. In this work, we try to examine the microstructural effect, on the corrosion resistance of some grades of carbon steel when they are subject to corrosion in alkaline soil, by the evaluation of the nature and properties of passive film formed on the surface of samples. In order to characterize the best resistance to corrosion of these grades steel, several electrochemical techniques were used, such as the potentiodynamic polarization curves, weight-loss, and polarization resistance. Electrochemical impedance Spectroscopy (EIS), Fourier transforms infrared (FTIR), SEM-EDX, and X-ray techniques were used to characterize the phase constituents of the rusts and to deduce long-term corrosion behavior of steel.

Experimental part

The test samples were fabricated from pipes of API 5L X42, X52, X60, and X70 steel. They had been used extensively in high pressure natural gas transmission in Algeria. They come from different manufacturers, and they were subjected to different thermomechanical treatments. Therefore, it presents a noticeable difference in their microstructures. Materials have been chosen as representative of tubes posed on the line past ten year, where corrosion and corrosion cracks were detected. Chemical compositions of both steels were listed in Table 1. The surfaces of 1 cm² were polished in the manner usually practiced in metallography. This involves polishing them with ever finer polishing material, ending with alumina of less than 0.3 µm of size, and etched with 2% nital before being examined with optical microscope and scanning electronic (SEM). The samples were characterized in terms of their elemental composition and microstructure. The test solution was a soil-extracted solution (NS4), consisting of 483 mg/l NaHCO₃, 122 mg/l KCl, 181 mg/l CaCl₂, and 131 mg/l MgSO₄·7H₂O. All the tests were performed at ambient temperature

Table 1: Chemical components of the steels used in the tests (W. %)

Dés	Fe	Cr	Ni	Mn	Si	Cu	Co	V	S	P	Ti	Al	Mo	Nb	C
X42	98.3513	0.0022	0.0166	0.6797	0.2219	0.3143	0.0203	0.0043	0.0136	0.0105	0.0025	0.0188	0.0363	-	0.1395
X52	98.2475	0.0032	0.0017	1.2888	0.1436	0.0215	0.0126	0.0040	0.0186	0.0015	0.0022	0.0399	-	0.0564	0.1740
X60	97.9328	0.0018	0.0011	1.0760	0.2334	0.1250	0.0220	0.0563	0.0123	0.0028	0.0041	0.0257	0.0948	0.0151	0.1250
X70	97.5048	0.0054	0.0622	1.6648	0.3152	0.0213	0.0159	0.0665	0.0091	0.0089	0.0039	0.0343	-	0.0321	0.1722

Electrochemical measurements were performed in a three electrode cell using an EGG Model 273A potentiostat. Pipe steel electrode was used as working electrode, a platinum wire as counter electrode and a saturated calomel electrode (SCE) as reference electrode. During polarization curve measurements, the potential scan rate was 20mV/s. The Ohmic potential drop was compensated by the instrument. During EIS measurements, an AC disturbance signal of 10 mV was applied on the electrode at open-circuit potential. The measuring frequency ranged from 10^5 to 0.01 Hz. Furthermore, scanning electron microscopy (PSEM) was used to observe the surface morphology before and after corrosion tests, and the corrosion products were analyzed by electron probe microanalysis (EPMA) in energy dispersion mode (EDX) for elemental composition, X-ray diffraction patterns (XRD), and Fourier transforms infrared (FTIR).

Results

1. Mechanical proprieties and microstructure observation

It is important to note that the phases present are mainly determined by elemental composition, thermal and mechanical history [14]. Chemical analysis revealed that the elemental composition of the steel samples was very similar. It is worth noting that all samples did not contain significant levels of Chromium, Nickel and Molybdenum, where as the Phosphorus and Sulfur levels are well below the maximum limits set by the 5L specification. The higher X grade materials (X60 and above) comprised notable levels of the grain-refining elements Niobium and Vanadium. Titanium and Aluminum, which are also known to refine grain size, were detected in some samples. Refining of the grain size is desirable since it is the only structural change that concurrently increases both strength and toughness [15].

The low carbon and alloy contents of steels suggest that they can be expected to have predominantly ferritic constituent [16]. The microstructure of X42 (Fig.1a) has a ferrite/pearlite structure (pearlite dark areas, and ferrite white areas), and the pearlite phase is uniformly distributed within the ferrite matrix. This sample has a smaller pearlite volume fraction (61.9% ferrite, and 39.1% pearlite) and a larger grain size compared to the other samples (20 – 30 μm). The X52 sample (fig.1b) has a ferrite-pearlite microstructure (49.3% ferrite / 50.7% pearlite), the grains size is smaller compared to the X42 steel, and it's ranging between 5 and 10 μm . The X60 structure (fig. 1c) consists of 41.3% of ferrite and 55.8% of pearlite, with a minor amount of bainite. The grains size varies between 10 and 15 μm . A microstructure of X70 sample (fig.1d) is consisted of the acicular ferrite, pearlite, and martensite (40.8% ferrite/ 53.5% pearlite). The very fine grains size is observed, and no inclusions or pores were visible in this sample.

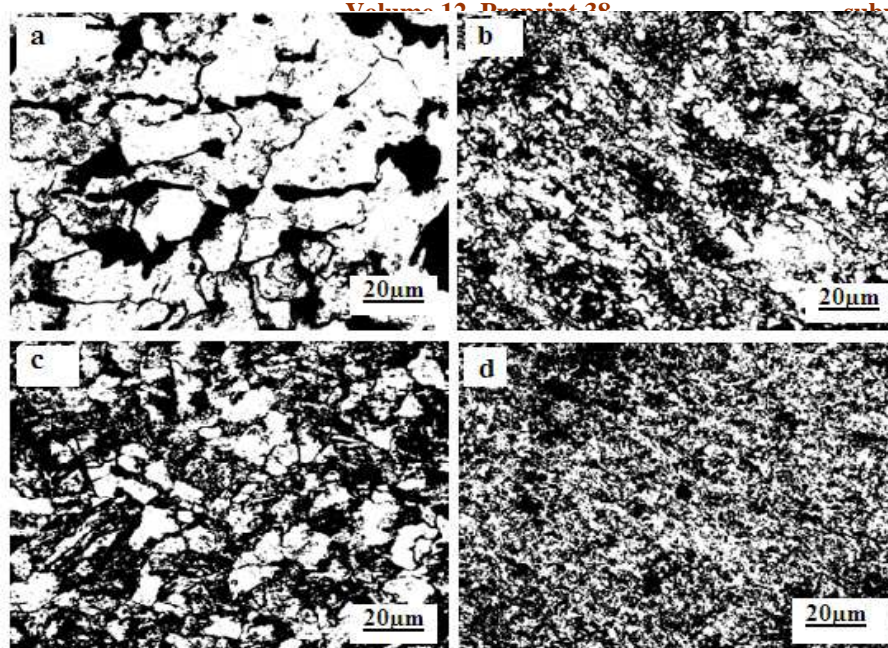


Fig. 1 Metallographic views of the microstructures of API 5L X42 (a), X52 (b), X60 (c), X70 (d) steel sample

2. Electrochemical Tests

The polarization curves obtained after 30 min of immersion in NS4 soil solution shows that the behavior of the samples (X42, X52, X60 and X70) is generally governed by a mechanism of activation. Thus we can assess the corrosion potential (E_{corr}) and the corrosion current density (I_{corr}) from plot of Tafel lines for which the anodic and cathodic branches show that the corrosion reaction under thermodynamic control nondiffusional. By comparing the variation of the corrosion current density, corrosion potential, and the anodic and cathodic Tafel slope (table.2), this shows that the corrosion of carbon steel is affected by microstructure.

Table 2: Polarization parameters for the corrosion of low carbon steel in soil test solution

Steel samples	E_{corr} (mV)	I_{corr} ($\mu\text{A}/\text{cm}^2$)	b_c (mV/deca)	b_a (mV/deca)
X52	-690.5	4.01	-275.18	516.41
X70	-702	3.01	-297.15	438.30
X60	-703.4	2.08	-303.91	436.91
X42	- 697	0.44	-307.41	398.73

3. Corrosion rate results

Corrosion rates of carbon steel samples measured by polarization resistance and weight-loss have been summarized in figure 3. The X42 steel sample present the lowest corrosion rate compared with those of X60, X70 and X52. This reflects clearly the relationship between the microstructure of the material and its resistance to corrosion.

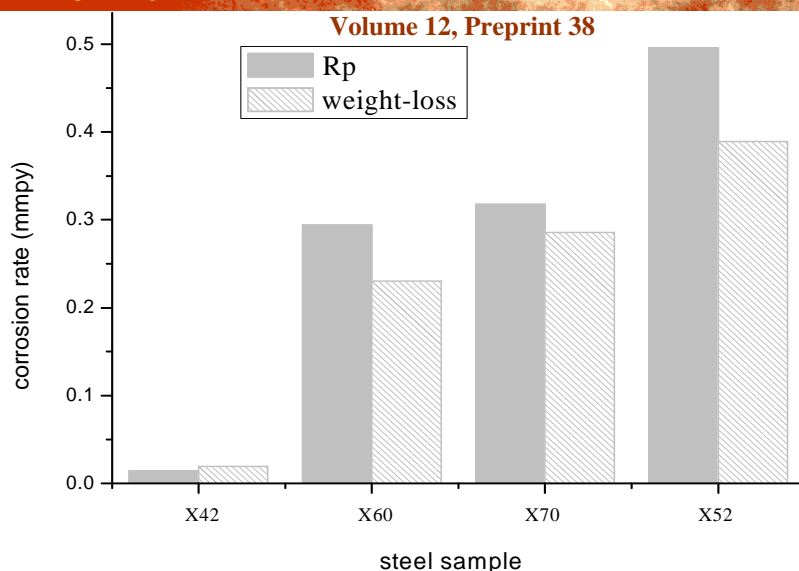


Fig. 2 Corrosion rate of various carbon steel samples buried in soil for 30 days, measured by weight-loss, and polarization resistance

4. EIS measurements

Figure 3 shows the Nyquist diagrams measured on the exposed surface of the carbon steel samples in NS4 solution. It is apparent that there are quite different impedance features for each sample. The impedance curves were dominated with one time constant only, i.e., a semicircle over the whole frequency range, and the size of the high-frequency decreased with a semicircle when moving from a coarse microstructure to a fine microstructure.

An electrochemical equivalent circuit that contains a solution resistance, R_s , in series with a parallel circuit of charge-transfer resistance, R_t , and constant phase element (CPE) for the double charge layer, was used to fit the impedance data. The largest charge-transfer resistance was recorded for the X42 steel, compared with that of the other samples. This decreasing resistance could be caused by the instability of the oxide layers or by the porosity.

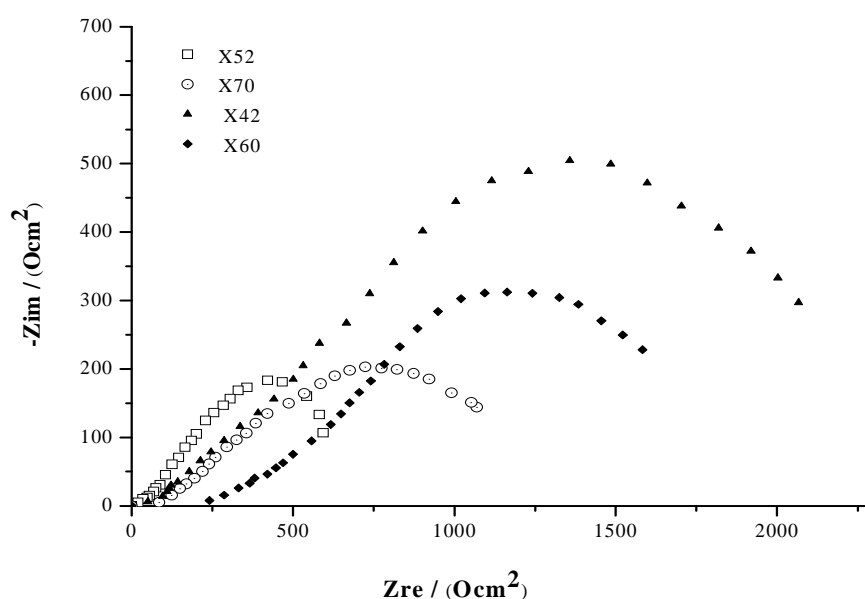


Fig. 3 Nyquist plots of low carbon steel samples that immersed in NS4 soil solution

Examination under a scanning electron microscope (SEM) of surface before and after the attack in NS4 soil solution will reveal the presence of corrosion products on the surface of samples (Figure 4). On the surface of the X42 sample, the layer is compact and uniformly covered the surface. While for X52, X60 and X70 corrosion products formed are porous and defective, or do not cover the entire surface. The corresponding energy spectrum (Fig 4) shows that these products are made of a number of chemical elements whose majority is iron and oxygen (Table 3). From the peaks of iron, corrosion products consist principally of iron oxide. Indeed, the iron peaks are large indicating that the iron is not under an individual but it is combined with other chemicals, probably oxygen and hydrogen

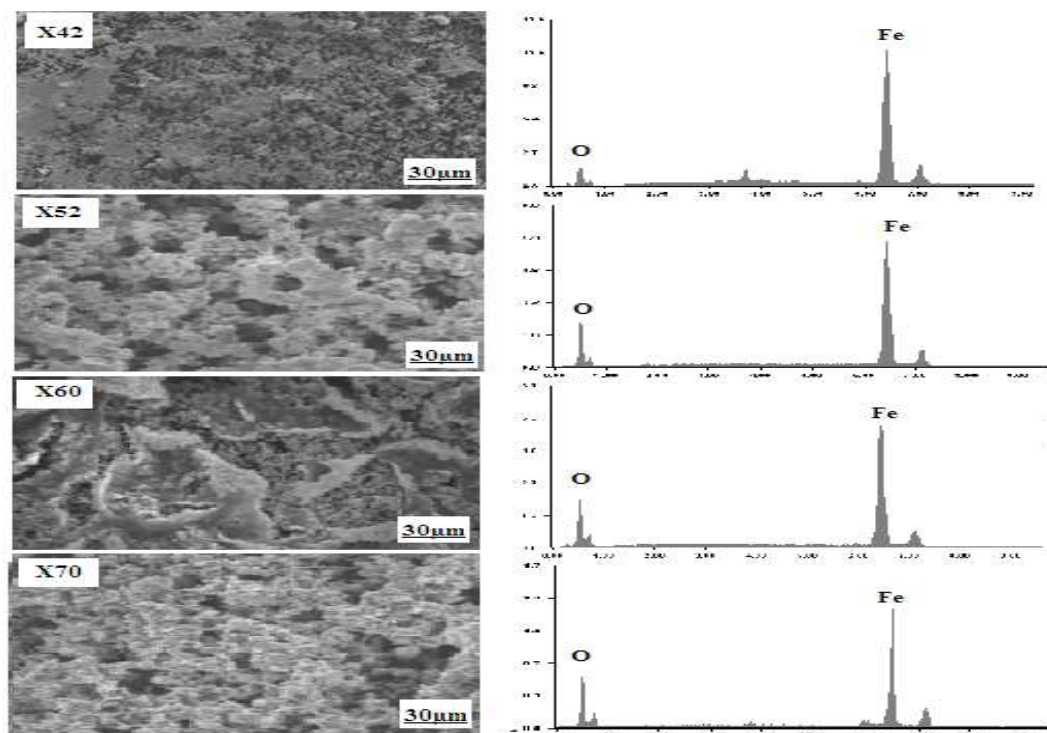


Fig. 4 The surface morphology and the energy dispersive (EDX) spectra of low carbon steel samples exposed for 40 day to soil test solution

Table 3: Chemical composition of the samples surface determined by EDX after corrosion (W %).

Pipe samples	Fe	O
X42	87.30	9.57
X52	80.44	19.56
X60	69.19	24.25
X70	74.33	22.13

It can also be seen in figure 5 that the FTIR spectra corresponding to different carbon steel samples were similar. The layers formed on the steel surfaces are composed of a mixture of goethite (α -FeOOH), lepidocrocite (γ -FeOOH) and δ -FeOOH. Goethite had peculiar peaks at 885 cm^{-1} and 780 cm^{-1} , and lepidocrocite had peaks at 1020 cm^{-1} , 750 cm^{-1} and 1450 cm^{-1} , while the amorphous δ -FeOOH had peaks at 1124 cm^{-1} and 794 cm^{-1} . The FTIR spectra of the relevant phases can be found in the literature [17, 18]. The peak at

3120 cm^{-1} is the O-H stretch vibration from lepidocrocite, and the peak at 3380 cm^{-1} is the O-H stretch vibration from δ -FeOOH [19, 20]. The peak of δ -FeOOH is almost invisible in the case of X42 samples.

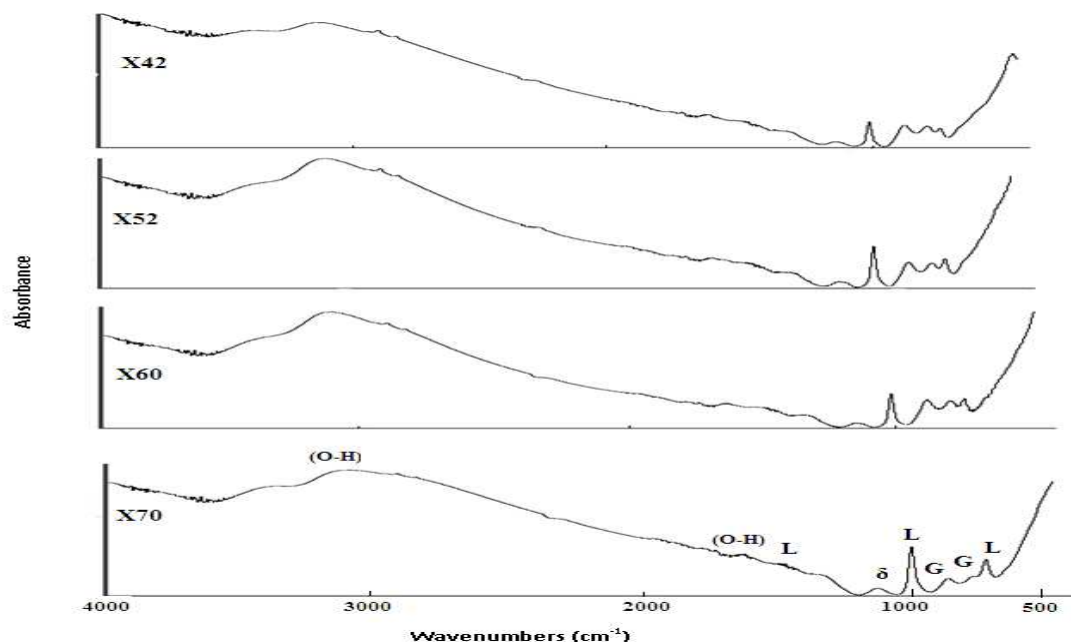


Fig. 5 FTIR spectra of the low carbon steel samples corroded by NS4 soil solution during 40 days (G: goethite, L: lepidocrocite, γ : γ -FeOOH)

The XRD data were used to support the FTIR spectra results. The composition of corrosion products on the various steels determined by XRD analysis is shown in figure 6. According to the XRD analysis results, the rust mainly consisted of the following phases: goethite (α -FeOOH), lepidocrocite, and iron oxide FeOH_3 , the γ -FeOOH is invisible.

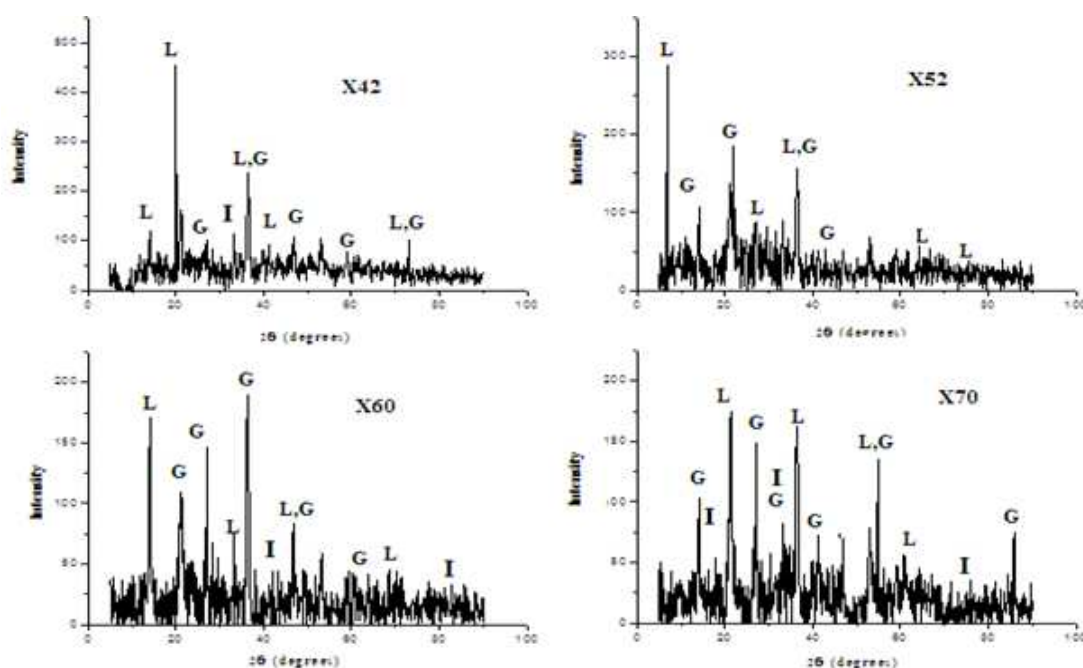
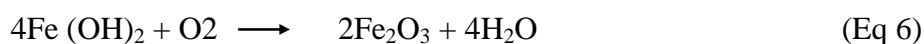
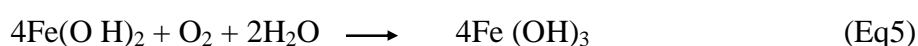
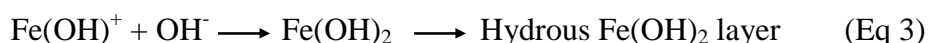
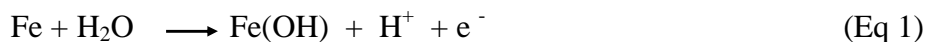


Fig. 6 XRD characterization of corrosion products formed on surface steel samples after 40 days of test in soil solution (G: goethite, L: lepidocrocite, γ : γ -FeOOH)

In the presence of an electrolyte such as water, corrosion reactions of low carbon steel are dominated by the Oxygen reduction and iron oxidation. The anodic process is described as a multiple-step oxidation reaction of iron with the formation $\text{Fe}(\text{OH})_2$, then FeOOH [21, 22]:



Based on our results, all iron oxides as suggested in Eq 1-7 are possible in aerated alkaline soil solution. XRD, FTIR, and SEM results showed the presence of corrosion products on the all samples surfaces, with almost the same chemical composition, and different structures and morphologies. Generally, the passive layer is a stable film; it can block the corrosives species approaching of the surface samples, and to inhibit the further corrosion of steel. The present work shows that a stable passive region could not be developed on all the samples studied. Indeed, the deposit layer formed on X42 steel is compact, and inhibits effectively the steel corrosion. However, the deposit layer formed on the surface of X52, X60, and X70 steel are porous and defective, and does not effectively protect the steel. These samples have a very low resistance to corrosion compared to X42 steel.

Our experiments have shown that the steel microstructure affects the properties of oxide layers. Perhaps the most significant of these properties are adherence of the film, and its power protector. The use of new manufacturing processes and application Heat treatment lead to changes in the structure of carbon steels, and improves their mechanical properties. But in the case of our samples, these transformations have not made a significant improvement in their resistance to corrosion. We observed that the structure is more improved, more corrosion resistance is weakened. In addition, the passive layer that normally protects steel becomes porous and poorly adherent, and it can accelerate the corrosion process.

The choice of a steel grade cannot be carried out only for these mechanical properties, but must take into account the properties of the oxide layer that forms when the pipe is buried in soil. It is necessary even useful to determine the process of formation and transformation of these oxides in this environment. Because this layer can form an effective protection, or aggravated the corrosion process.

Conclusion

The present work shows that corrosion of steel is affected by its microstructure, and its mechanical properties. The nature of passive films formed on metals is the ultimate factor which controls their corrosion behavior. The laboratory experiments realized have shown that the microstructure influences the properties of the corrosion layers, such as morphology, proportion of the various chemical compounds present, the protective properties and adherence of the film for carbon steels with apparently the same composition. It can lead to the formation of a passive layer, compact that inhibits effectively, or the formation of a fragile and unstable layer, that promotes the destruction of the material in the long term.

References

- [1] American Petroleum Institute, 'API Specifications 5L', 41st edn. (1995).
- [2] S. Nasu, T. Kamimura, T. Tazaki, *Hyperfine Interactions* 139/140 (2002), 175
- [3] A. V. Ramesh Kumar, R. Singh, R. K. Nigam, J. *Radioanal. Nuc. Chem.*, 242, 1 (1999), 131
- [4] L. Chang, and S. Ning Lin, *Oxidation of Metals*, 63(2005), 131
- [5] E. Kh. Enikeev, A. K. Feoktistov, M. K. Panov, and I. M. Krashennnikova, *Russ. J. Electrochem.*, 4, 36(2000), 378
- [6] Richard S. Perkins, James D. Garber, *J. Sol. Chem.*, 32, 3(2003), 265
- [7] A. Samide, I. Bibicu, M. S. Rogalski, M. Preda, *J. Radioanal. Nuc. Chem.* 261, 3 (2004), 593
- [8] S. I. Hirnyi, *J. Mat. Sci.*, 37, 1(2001), 87
- [9] Y. Wan, C. Yan, *J. Mat. Sc.*, 38 (2003), 3597
- [10] D.C. Cook, S.J. Oh, R. Balasubramanian, and M. Yamashita, *Hyperfine Interactions* 122 (1999), 59
- [11] L. Zhang, X.G. Li, C.W. Du, and Y.F. Cheng, *J. Mat. Eng. And Perf.* 18 (2009), 319–323
- [12] L. Freire, X.R. Nóvoa, M.F. Montemor, M.J. Carmezim, *Mat. Chem. and Phys.*, 114 (2009), 962–972
- [13] A. Benmoussa, M. Hadjel, M. Traisnel, *Mat. and Corr.* 57,10 (2009), 771-777
- [14] R.A. Higgins, *Appl.Phys. Met.*, 6th. edn. (Arnold, London, 1993).
- [15] H.E. McGannon (Ed.), 'The Making, Shaping and Treating of Steel', 9th edn. (United States Steel, 1971).
- [16] L.E. Samuels, 'Optical Microscopy of Carbon Steels' (ASM, 1980)
- [17] A. Raman, B. Kuban, and A. Razvan, *ibid.* 32, 12 (1991), 1295
- [18] T. Misawa, K. Asami, K. Hshimoto and S. Shimodaira, *ibid.* 14 (1974), 279
- [19] M. Yamashita, H. Miyuki, Y. Matsuda, H. Nagano, and T. Misawa, *ibid.* 36, 2, (1994), 291.
- [20] J. G. WU, *Sci. Tech. Inf. Press, Beijing*, 2 (1994), 271.
- [21] Y.F. Cheng and J.L. Luo, *Electrochimica Acta*, 44, (1999), 4795–4804
- [22] B.R. Tian a, Y.F. Cheng, *Corros. Sci.*, 50, (2008), 773–779